HHS Public Access

Author manuscript

Nat Chem Biol. Author manuscript; available in PMC 2012 June 01.

Published in final edited form as:

Nat Chem Biol. ; 7(12): 909–915. doi:10.1038/nchembio.690.

GPCRs regulate the assembly of a multienzyme complex for purine biosynthesis

Florence Verrier[1,*], **Songon An**[2,*,#], **Ann M. Ferrie**[1], **Haiyan Sun**[1], **Minjoung Kyoung**[3], **Huayun Deng**[1], **Ye Fang**[1,**], and **Stephen J. Benkovic**[2,**]

[1]Biochemical Technologies, Science and Technology Division, Corning Inc., Corning, NY 14831

[2]Department of Chemistry, Pennsylvania State University, University Park, PA 16802

[3]Department of Molecular and Cellular Physiology, Stanford University, Stanford, CA, 94305

Abstract

G protein-coupled receptors (GPCRs) transmit exogenous signals to the nucleus, promoting a myriad of biological responses *via* multiple signaling pathways in both normal and cancer cells. However, little is known about the response in cytosolic metabolic pathways to GPCR-mediated signaling. Here, we applied fluorescent live-cell imaging and label-free dynamic mass redistribution assays to study whether purine metabolism is associated with GPCR signaling. By screening a library of GPCR ligands in conjunction with live-cell imaging of a metabolic multienzyme complex for *de novo* purine biosynthesis, the purinosome, we demonstrated that the activation of endogenous $G_{\alpha i}$-coupled receptors correlates with purinosome assembly/disassembly in native HeLa cells. Given the implications of GPCRs in mitogenic signaling as well as the purinosome in controlling metabolic flux *via de novo* purine biosynthesis, we hypothesize that regulation of purinosome assembly/disassembly may represent one of downstream events of mitogenic GPCR signaling in human cancer cells.

Keywords

G protein-coupled receptor; metabolism; protein complex; purine biosynthesis; purinosome

**Correspondence should be addressed to Y.F. (Fangy2@corning.com) and S.J.B. (sjb1@psu.edu).

*These authors contributed equally to the study.

#Current address: Department of Chemistry and Biochemistry, University of Maryland Baltimore County, 1000 Hilltop Circle, Baltimore, MD 21250

Note: Supplementary Information is available

COMPETING FINANCIAL INTERESTS

F. Verrier, A.M. Ferrie, H. Sun, H. Deng, and Y. Fang are employees and shareholders of Corning, Inc.

Author Contributions

F.V. and S.A. contributed equally to the study. F.V. performed DMR assays and analyzed DMR data. S.A. performed fluorescent live-cell imaging and initial DMR assays, and analyzed data. A.M.F. prepared the compound library and performed initial DMR assays. H.S. performed quantitative real-time PCR. M.K. designed and modified a fluorescent microscope for image collection. H.D. carried out DMR assays related to part of Figure 3b, part of supplementary DMR assays. Y.F. and S.J.B. conceived and designed the study, and analyzed data. S.A., Y.F., and S.J.B. wrote the manuscript.

Introduction

G protein-coupled receptors (GPCRs) are the largest family of membrane receptors that participate in cellular signal transduction to elicit a myriad of cellular responses[1,2]. GPCRs are traditionally viewed as transducers engaged in tissue-specific and post-mitotic functions in fully differentiated cells. However, the functions of many GPCRs particularly the $G_{\alpha q}$, $G_{\alpha i}$ and $G_{\alpha 12}$ proteins are oncogenic and promote cellular transformation and mitogenesis in various disease and experimental states[3,4].

Cell signaling through GPCRs relays messages derived from environmental ligands to intracellular effectors. The agonist-activated receptor can tune the action of second messengers through G-protein dependent pathway or activate G-protein independent pathways[5]. These signaling pathways propagate changes in the cellular nucleus that modulate the activities of various transcription factors. Elucidation of the members and interactions in such signaling pathways is analytically challenging.

Cellular metabolism is essential for cell proliferation, with abnormal metabolism a principal hallmark of human cancer[6]. Metabolic reprogramming in cancer occurs from enzyme levels to global genomic and proteomic alterations, that are often manifest in increased activities of oncogenic signaling pathways[7]. For instance, *de novo* nucleotide biosynthesis is often upregulated in cancer cells to provide building blocks for the synthesis of RNA, DNA and other effectors[8]. Small molecule inhibitors of *de novo* purine biosynthesis long have been used as drugs against cancer and inflammatory disorders[9]. However, nothing is known about the role of GPCR signaling in modulating *de novo* purine biosynthesis.

Recently, a reversible multienzyme complex participating in *de novo* purine biosynthesis, the purinosome, was discovered in human cell lines[10]. The purinosomes were dynamically regulated by inhibition of casein kinase 2 (CK2)[11] and spatially controlled by the matrix of microtubule filaments[12]. Independently, a cellular dynamic mass redistribution (DMR) assay had been developed to investigate cellular signaling pathways, especially GPCR-mediated transduction processes, with a capability of high-throughput screening[13–15]. DMR assays employ a resonant waveguide grating (RWG) biosensor to track the dynamic redistribution of cellular matter in real time within ~150 nm of the sensor surface, and convert it into a kinetic and integrated response (*i.e.* DMR signal) upon stimulation with a ligand[16]. DMR assays are rich in texture with wide pathway coverage so that endogenous receptors can be systematically studied. Further, DMR assays are flexible in assay formats and compatible with various chemical perturbations, thus enabling mechanistic deconvolution of signaling pathways downstream of a receptor.

By taking advantage of DMR assays in conjunction with fluorescent live-cell imaging (Fig. 1), we sought a correlation between reversible purinosome assembly and signaling of endogenous GPCRs. Our orthogonal approach utilizing both label and label-free technologies revealed that the activation of endogenous G_i-coupled receptors coincided with purinosome assembly/disassembly in native HeLa cells.

Results

DMR signatures correlated with purinosome reversibility

Our previous imaging study of the *de novo* purine biosynthetic pathway enzymes in HeLa cells reveals that the CK2 inhibitors, 2-dimethylamino-4,5,6,7-tetrabromo-1H-benzimidazole (DMAT), 4,5,6,7-tetrabromo-1H-benzimidazole and tetrabromocinnamic acid, promotes the formation of purinosomes, whereas 4,5,6,7-tetrabromobenzotriazole (TBB) causes a sequential biphasic transition; *i.e.* purinosome formation followed by its subsequent dissociation[11]. TBB can also dissociate purinosomes induced by DMAT with[11] or without removal of DMAT (Fig. 1b–d), indicating that the two inhibitors employ different mechanisms to affect purinosome formation. Additionally, siRNA knockdown of CK2α catalytic subunits leads to purinosome formation in HeLa cells[11].

We now tested all four inhibitors in DMR assays. At 32 μM all gave a biphasic DMR signal – an initial positive DMR (P-DMR) event followed by a decaying negative DMR (N-DMR) event (Supplementary Fig. 1). The common early P-DMR signal exhibited by all inhibitors suggests that they promote a similar intracellular event. However, the DMR signals of different inhibitors diverge in their dose responses. For DMAT: at low doses (*i.e.* <2 μM) the P-DMR plateau level was retained for > 2 hrs, whereas at high doses (*i.e.* >2 μM) the P-DMR became unsustainable (Supplementary Fig. 2). However, for TBB low doses (*i.e.* 1–8μM) only triggered a N-DMR, but high doses (*i.e.* > 8μM) primarily triggered a biphasic DMR with a short-lived small P-DMR event followed by N-DMR. The dose responses of DMAT and TBB provided EC_{50}s of 26 ± 8 nM (n=4; Supplementary Fig. 2) and of 9.9 ± 2.6 μM (n=4; Supplementary Fig. 2), respectively. The opposing DMR characteristics appear to correlate with their distinct effects on purinosome assembly/disassembly – the DMAT-induced DMR would signal purinosome association, whereas TBB-mediated DMR signals would correlate with the initial assembly then disassembly of the purinosome. DMAT and TBB are known to display distinct polypharmacology besides inhibiting CK2 activity[17,18]. Since the dose responses reflect their integrative pharmacology in HeLa cells, the biphasic response of DMAT at high doses may be associated with purinosome promotion (the early response) and other cellular effects such as toxicity via unknown mechanisms (the late response). Consequently, we reasoned that the DMR response to a sequential addition of the two inhibitors (*i.e.* DMAT followed by TBB, or *vice versa*) should have a greater possibility of reflecting the potentiation of purinosome assembly/disassembly that was observed by cellular imaging for the inhibitors.

We designed a two-step DMR assay in which cells were stimulated with the sequential addition of DMAT followed by TBB with no removal of the first before addition of the second. Results showed that the DMR signal induced by DMAT was reversed by subsequent TBB addition (Fig. 1e). Moreover, pretreatment of cells with one of the two inhibitors potentiated the DMR signals induced by the other (Fig. 1f). The cross-potentiation of the individual DMR signals (DMAT or TBB) by the other is consistent with their observed effect on purinosome assembly/disassembly in cellular imaging, further indicating that DMAT and TBB act through different mechanisms to regulate purinosome dynamics. Importantly, DMR assays with siRNA demonstrated that knockdown (~45%) of CK2α

catalytic subunits potentiated the TBB N-DMR but diminished the TBB early P-DMR (Fig. 1g), and suppressed the DMAT early P-DMR (Fig.1h).

DMR screening of GPCR agonists in HeLa cells

We then ran the DMR assay for a library of 115 compounds, 113 of which are GPCR agonists (Fig. 2, and Supplementary Table 1). The screening was carried out using 20μM DMAT followed by 25 μM TBB, in order to be consistent with live-cell imaging studies and to be compatible with the relatively short duration of DMR assays. The higher the dose, the more rapid the response is. Comparing to the negative control (*i.e.*, vehicle only), the assay was found to be robust for the early DMR of DMAT (Z' of 0.75; n =48), and the N-DMR of TBB (Z' of 0.81; n =48). Modulation of the DMR signals first from DMAT and then from TBB after pretreatment with GPCR agonists when plotted fell into four regions as shown by the different shaded colors in Figure 2. The majority of small molecules did not alter the DMR signatures of DMAT and TBB, and clustered near the positive control where the cells were not pretreated with any agonists before the subsequent additions of DMAT and TBB (also see Fig. 1e). However, five small molecules in the pink shaded area significantly affected both the DMAT and TBB responses. These molecules are epinephrine (EPI), clonidine, A61603, phenylephrine and dopamine, all of which are adrenergic receptor (AR) agonists. Other drugs in the yellow and blue shaded areas changed only the DMAT signal but not the TBB signal. Both prostaglandin E_2 (PGE_2) and D_2 (PGD_2) are known agonists for prostaglandin EP and FP receptors; lysophosphatidic acid (LPA) is the natural agonist of LPA receptors; and UDP, ADP, ATP and UTP are known agonists for purinergic P2Y receptors. Consistent with the DMR assays, quantitative real-time PCR revealed that native HeLa cells endogenously express mRNAs for α_{2A}-AR (cycle threshold, C_t, 23.9), β_2-AR (C_t, 23.9), $P2Y_1$ (C_t, 28.5), $P2Y_2$ (C_t, 26.3), $P2Y_6$ (C_t, 27.0), $P2Y_{11}$ (C_t, 28.6), LPA_1 (C_t, 27.9), LPA_2 (C_t, 27.4), LPA_5 (C_t, 27.3), EP_4 (C_t, 25.7), and FP (C_t, 28.0) receptors. However, little or no mRNAs were detected for α_{1A}- (C_t, 37.1), α_{1B}- (C_t, 30.4),α_{1D}- (undetected), α_{2B}-(C_t, 33.5), α_{2C}- (C_t, 33.4), β_1- (C_t, 32.7), and β_3-ARs (C_t, 38.5). Similarly, little or no mRNAs were detected for $P2Y_4$ (Ct, 33.6), $P2Y_5$ (Ct, 31.1), $P2Y_8$ (undetected), $P2Y_{10}$ (undetected), $P2Y_{12}$ (undetected), $P2Y_{13}$ (undetected), $P2Y_{14}$ (Ct, 35.6), LPA_3 (Ct, 31.2), LPA_4 (Ct, 33.3), DP (undetected), IP (undetected), EP_1 (Ct, 32.2), EP_2 (Ct, 29.5), and EP_3 (34.2) receptors. As controls, cycle threshold values for hypoxanthine phosphoribosyltransferase 1 and glyceraldehyde-3-phosphate dehydrogenase were found to be 20.6 and 15.4, respectively.

We chose to focus on AR receptors because i) AR agonists generated the most significant signal changes upon addition of both DMAT and TBB, ii) AR agonists induced robust and relatively simple DMR traces with significant detection windows (see below), and iii) HeLa cells endogenously express both α_{2A}- and β_2-ARs, which are two prototypic GPCRs that mediate distinct signaling pathways.

Deconvolution of signaling pathways via endogenous ARs

Although the β_2-AR is considered to be a prototypic $G_{\alpha s}$-coupled receptor and the α_{2A}-AR a $G_{\alpha i}$-coupled receptor[19,20], we first investigated whether the DMR assay was capable of distinguishing distinct G protein-coupled signaling pathways in HeLa cells using specific

agonists and antagonists for each AR. Oxymetazoline (OXY), a selective agonist for α-ARs relative to β-ARs, triggered a dose-dependent P-DMR signal with an EC_{50} of 3.8 ± 1.2 nM (n=6) and a maximal amplitude of 186 ± 11pm (n = 6) (Fig. 3a, and Supplementary Fig. 3a). UK14304, a full α_2 agonist, led to a P-DMR with an EC_{50} of 1.8 ± 0.2 nM (n =4) and a maximal amplitude of 271 ± 17 pm (n = 4) (Fig. 3a, and Supplementary Fig. 3b). Salmeterol (SAL), a β_2-AR strong partial agonist, also led to a dose-dependent P-DMR signal with an EC_{50} of 19.0 ± 4.2 nM (n=6) and a maximal amplitude of 74 ± 9 pm (n=6) (Fig. 3a, and Supplementary Fig. 3c). Isoproterenol, a selective agonist for β-ARs relative to α-ARs, resulted in a P-DMR signal with EC_{50} of 548 ± 35 nM (n = 4) and a maximal amplitude of 103 ± 8 pm (n =4) (Fig. 3a, and Supplementary Fig. 3d). The AR pan agonist, epinephrine, resulted in a P-DMR signal with an EC_{50} of 15.0 ± 3.7 nM (n = 6) and a maximal amplitude of 434 ± 39 pm (n =6) (Fig. 3a, and Supplementary Fig. 3e). At saturating doses, the epinephrine DMR was greater than the simple sum of both oxymetazoline and isoproterenol signals (Fig. 3a). In short, we were able to obtain differential agonist-dependent optical traces in the DMR assays upon activation of different subclasses of the ARs.

We then challenged the cells with the AR agonists in the presence of antagonists. The co-stimulation with either betaxolol or propranolol, two β-blockers[21], only slightly suppressed the epinephrine signal (Fig. 3b). Co-stimulation with either phentolamine or yohimbine, two α_2-AR-selective antagonists, markedly suppressed the epinephrine signal (Fig. 3b). Co-stimulation with 1μM prazosin, a potent α_1-selective antagonist, had no impact on the epinephrine signal (Fig. 3b). Co-stimulation with propranolol and yohimbine completely blocked the epinephrine signal (Fig. 3b). We deduced from these agonist and antagonist data that the DMR signal from epinephrine is primarily derived from activation of the α_{2A}-AR, and to a smaller degree from activation of the β_2-AR receptor. In addition, yohimbine completely inhibited the DMR signal induced by oxymetazoline and clonidine, and only partially attenuated the DMR signal induced by A61603, dopamine and phenylephrine (Fig. 3c), suggesting that both oxymetazoline and clonidine are specific to the α_{2A}-AR in HeLa cells, and the latter three agonists activate receptors besides the α_{2A}-AR.

Next, we carried out toxin experiments to decode the pathways downstream of the epinephrine response. It is known that pertussis toxin (PTX) binds to $G_{\alpha i}$, resulting in permanent inhibition of $G_{\alpha i}$ by ADP ribosylation of a Cys residue and decoupling of the G protein from the receptor[22]. Cholera toxin (CTX) binds to $G_{\alpha s}$, resulting in permanent activation of $G_{\alpha s}$ by ADP ribosylation of an Arg residue and cAMP production[23]. The ADP ribosylation of $G_{\alpha s}$ protein with CTX only partially attenuated the epinephrine signal, which is similar to the effect of betaxolol and propranolol (Fig. 3d *vs*. Fig. 3b). However, silencing of $G_{\alpha i}/G_{\alpha o}$ proteins with PTX converted the epinephrine signal into a classic G_s-type DMR signal (Fig. 3d)[13], that is similar to the effect of the selective α_{2A}-AR antagonists, phentolamine or yohimbine (Fig. 3b). The DMR signal of salmeterol was significantly attenuated in CTX-treated cells, but not in PTX-treated cells (Fig. 3e), revealing that the permanent activation of $G_{\alpha s}$ protein by CTX overrides the activation of $G_{\alpha s}$ through the β_2-AR.

Collectively, we confirmed that HeLa cells indeed endogenously express functional ARs, and the α_{2A}-AR-stimulated DMR signal is largely downstream of the $G_{\alpha i}$ activation while

the β_2-AR DMR signal is mostly downstream of the $G_{\alpha s}$ activation. The residual DMR signals after toxin pretreatment (Fig. 3d-e) also suggest that G protein-independent signaling may contribute to the DMR signals induced by these ligands.

α_{2A}-AR agonists promoted purinosome assembly

According to the library screening results (Fig. 2), we hypothesized that the altered pattern in DMRs arising from DMAT and TBB in the AR-agonist-activated cells would reflect purinosome assembly induced by the AR-agonists. We conducted fluorescent live-cell imaging with HeLa cells transiently expressing green fluorescent protein (GFP)-conjugated human formylglycinamidine ribonucleotide synthase (hFGAMS) as a purinosome marker[10]. Treatment of HeLa cells grown in purine-rich medium with oxymetazoline (100 nM) indeed promoted purinosomes in the cytoplasm (Fig. 4a–b). Moreover, a ten-fold higher dose (1 μM) of salmeterol did not induce purinosome assembly on the same time scale (Fig. 4c–d). It is important to note that the cellular imaging for the two agonists was carried out at the levels that saturated their respective DMR signals (Supplementary Fig. 3f).

Next, we carried out DMR assays initiated with epinephrine, oxymetazoline or salmeterol, then followed by DMAT and TBB. Pre-activation of the α_{2A}-AR receptors with oxymetazoline or epinephrine attenuated DMAT signals (Fig. 5a), but potentiated TBB signals (Fig. 5b). These results suggest that α_{2A}-AR activation prior to DMAT addition already significantly facilitated purinosome formation, thus causing desensitization to the succeeding DMAT stimulation but sensitizing the TBB-induced purinosome disassembly. Moreover, pre-activation of the β_2-AR with salmeterol did not alter either DMAT or TBB signals (Fig. 5c and Fig. 5d, respectively).

Lastly, we performed the dose responses using DMR assays to study the correlation between receptor activation and the TBB mediated signaling. Epinephrine led to a dose dependent DMR with an EC_{50} of 15.0 ± 3.7 nM (Fig. 3a, and Supplementary Fig. 3e). The pretreatment with epinephrine also dose-dependently increased the TBB DMR (Supplementary Fig. 4a) with an EC_{50} of 4.0 ± 0.4 nM (n =4) (Supplementary Fig. 4b). Taken together with additional DMR assays carried out in the presence of various AR antagonists (Supplementary Fig. 4–5), both live-cell imaging and DMR assays supported purinosome formation by the α_{2A}-AR activation, but not by the β_2-AR stimulation, and provided compelling evidence that the α_{2A}-AR initiates a signaling pathway that correlates with purinosome assembly in HeLa cells.

$G_{\alpha i}$ signaling plausibly associated with purinosome

We next examined whether $G_{\alpha i}$ activation is required for transferring signals from the α_{2A}-AR to affect the purinosome. Firstly, DMR assays showed that silencing $G_{\alpha i/o}$ with PTX or ADP-ribosylating $G_{\alpha s}$ with CTX did not alter either DMAT or TBB signals in the absence of GPCR agonists (Supplementary Fig. 6). We interpret this result to mean that neither DMAT nor TBB affect purinosome assembly/disassembly through upstream G proteins. However, silencing $G_{\alpha i/o}$ with PTX almost completely blocked the oxymetazoline-caused DMR signal (Fig. 6a). Further, treatment by PTX almost completely blocked the oxymetazoline-caused desensitization of the succeeding DMAT stimulation (Fig. 6b),

suggesting that PTX prevents the α_{2A}-AR-activated purinosome formation by oxymetazoline. ADP-ribosylation of $G_{\alpha s}$ with CTX marginally attenuated the oxymetazoline-mediated DMR signal (Fig. 6a) and had little impact on the agonist-induced desensitization of the succeeding DMR stimulation (Fig. 6b). In TBB-induced signals (Fig. 6c), PTX prevented the oxymetazoline-induced sensitization of the succeeding TBB stimulation (in the presence of PTX fewer purinosomes are present for TBB-mediated disassembly), whereas CTX had little impact. Epinephrine also displayed effects similar to oxymetazoline did (Supplementary Fig. 7d–e).

To support our hypothesis we examined by imaging the effect of $G_{\alpha i}$-mediated signaling with transfected HeLa cells in the presence of PTX. As mentioned above, without PTX treatment, oxymetazoline induced purinosome assembly in transfected HeLa cells grown in purine-rich medium (Fig. 4a–b). However, for PTX-treated HeLa cells oxymetazoline did not promote purinosome assembly (Fig. 6d–e). Taken together, the $G_{\alpha i}$-mediated cascade was linked to purinosome formation through the α_{2A}-AR activation.

$G_{\alpha i}$ signaling generally regulated purinosome dynamics

As shown in Figure 2, purinergic P2Y receptors, LPA receptors and prostaglandin receptors likely participate in purinosome regulation. Briefly, purinergic P2Y receptor agonists (*i.e.* ATP, ADP and UDP), a LPA receptor agonist (*i.e.* LPA), and prostaglandin receptor agonists (*i.e.* PGE2 and PGD2) resulted in robust but distinct DMR signals (Supplementary Fig. 7), all of which were sensitive to both PTX and CTX pretreatments. These results are consistent with the ability of P2Y, LPA and prostaglandin receptors to activate multiple G protein-dependent signaling pathways. However, given their similarity to the α_{2A}-AR agonists (*i.e.* EPI and OXY in Supplementary Fig. 7d–e) in modulating the DMAT and TBB DMR signals, activation of these receptors by ATP, LPA and PGE2 (Supplementary Fig. 7d–e) implicates $G_{\alpha i}$ activation. In contrast, many other GPCR agonists in the library that also led to detectable DMR traces did not alter the DMAT and TBB signals (Fig. 2). Adenosine is a natural agonist of the endogenous G_s-coupled adenosine A_{2B} receptor (C_t of 23.9), histamine is a natural agonist of the endogenous G_q-coupled histamine H_1 receptor (C_t of 24.9), SFLLR and SLIGKV are synthetic agonists of the endogenous G_q-coupled protease activated receptor 1 (C_t of 26.1) and 2 (C_t of 27.1), respectively. Taken together, these results suggest that activation of various distinct receptors may differently regulate purinosome but the signal flows through a $G_{\alpha i}$ – mediated pathway.

Discussion

Multiple enzymes involved in *de novo* purine biosynthesis form a reversible purinosome assembly in live cells by changing purine levels in the growth media[10] or by applying small molecules to manipulate the activity and expression of protein kinase CK2[11]. Further, the purinosome formation is associated with an increased rate of purine biosynthesis[12]. Interestingly, opposing pharmacological effects observed with DMAT and TBB on purinosome assembly imply that at least one of these two active kinase inhibitors may intervene with different cellular targets, besides CK2, to regulate purinosome reversibility. In turn, we hypothesized that cells must sense physiological changes occurring in the growth

environment to regulate purinosome assembly, implying likely control by cellular signaling pathways.

Here we combined direct fluorescent live-cell imaging and indirect DMR assays to demonstrate that an agonist binding to the α_{2A}-AR and thus activating $G_{\alpha i}$ – mediated signaling pathway is associated with purinosome formation in live HeLa cells. We first showed that the DMAT- and TBB-induced DMR signals were correlated with the results of live-cell imaging that track purinosome assembly and disassembly. Secondly, using pharmacological agents we observed significant changes in DMR signals arising from DMAT/TBB with known AR agonists. Thirdly, interrogation of the DMR response with agents specific for the α_{2A}-AR or β_2-AR, e.g. oxymetazoline *versus* salmeterol, coupled with fluorescent live-cell imaging supported purinosome formation is associated with α_{2A}-AR but not β_2-AR activation. Finally, we showed that the DMR signals resulting from oxymetazoline were blocked by PTX but not CTX as revealed by alterations in both DMAT- and TBB-induced DMR signals. Importantly, this result was verified by fluorescent live-cell imaging. Collectively, we concluded that signals from the α_{2A}-AR that flow through $G_{\alpha i}$ induce purinosome assembly.

From our data, however, we cannot conclude whether CK2 directly or indirectly participates in the purinosome-associated $G_{\alpha i}$ coupled pathway because PTX does not alter DMR signals arising from DMAT or TBB in the absence of AR agonists. Experimental evidence for direct participation by CK2 in GPCR signaling has been sparse in the literature, except for a few reports focusing on specific subfamilies of GPCRs[24–27]. Activation of $G_{\alpha i}$ protein causes a $G_{\beta\gamma}$ subunit of the heterotrimeric G protein complex to interact with a lipid kinase, phosphatidylinositol-3-kinase (PI3K) whose signaling pathways include protein kinase B (*i.e.* Akt) in various cellular functions[25]. Since the activities of PI3K and Akt are regulated by CK2 through phosphorylation, they might participate in cellular signaling for purinosome assembly/disassembly. Additionally, since CK2 can be activated by the Wnt/β-catenin signaling pathway *via* a PTX-sensitive $G_{\alpha o}$ protein[28], the Wnt/β-catenin pathway may regulate purinosome dynamics as well. Nevertheless, our discovery constitutes a signaling pathway for purinosome regulation that addresses how a metabolic macromolecular complex operating for *de novo* purine biosynthesis is tightly associated with a cellular signal transduction in cells. We envision that complete understanding of the purinosome-associated GPCR pathway might constitute a new class of pharmacological targets and/or provide deeper understanding of existing drugs targeting GPCR signaling pathways. Our orthogonal approach combining label and label-free methods was for the first time able to provide compelling evidence for an intimate relationship between GPCR signaling and purine biosynthesis. The regulation of purinosome assembly/disassembly by GPCRs may represent one of downstream events of mitogenic GPCR signaling in human cancer cells.

Methods

Cloning and Materials

The plasmid expressing a *de novo* purine biosynthetic enzyme, hFGAMS, with monomeric enhanced green fluorescent protein (GFP) was prepared using a pEGFP-N1 vector (Clontech, CA) with two restriction enzymes, NheI and EcoRI (New England Biolabs, MA)

as described before[10]. Small molecules and peptides listed in Supplementary Table 1 were obtained from Sigma Chemical Co. (St. Louis, MO), Bachem (King of Prussia, PA) or Tocris (St. Lois, MO). CTX and PTX were obtained from Sigma. The remaining small molecules were obtained from vendors specified in Supplementary Table 2. Epic® 384well biosensor cell-culture compatible microplates (Corning Inc., Corning, NY) were obtained and used directly.

Transfection of Mammalian Cells

Human cancer cell line HeLa (ATCC, Manassas, VA) was maintained and transfected for this study as described before[10]. Briefly, we subjected these cell lines to both purine-rich medium: Minimal Essential Medium (MEM; Mediatech), 10% fetal bovine serum (FBS; Atlanta Biological) and 50 μg/mL gentamicin sulfate (Sigma); and purine-depleted medium: Roswell Park Memorial Institute 1640 (RPMI 1640; Mediatech) supplemented with dialyzed 5% FBS and 50 μg/mL gentamicin sulfate. FBS was dialyzed against 0.9% NaCl at 4°C for ~2 days. Lipofectamine™ 2000 (Invitrogen) as a transfection reagent was used by following the manufacturer's protocol. Unless otherwise indicated, hFGAMS-GFP was transiently expressed in HeLa cells as a purinosome marker.

Fluorescence Microscopy of Live Cells

All samples were imaged at ambient temperature (~25°C) with a 60 × objective (1.49 NA, Nikon Apo TIRF) using a Photometrics CoolSnap ES^2 CCD detector mounted onto a Nikon TE-2000E inverted microscope. GFP detection was accomplished using a S484/15x excitation filter (Chroma Technology), S517/30m emission filter (Chroma Technology) and Q505LP/HQ510LP dichroic (Chroma Technology). Nikon imaging software, NIS-Elements (version 3.0) was used for collecting and analyzing images. Small molecules were added to cells after washing at least 3 times with Hank's balanced salt solution (HBSS; Gibco). Images were acquired prior to drug addition and after cells had been incubated with drugs at various time points. PTX was directly added to reach a final concentration of 100 ng/ml and incubated for 6 hrs prior to imaging. The final concentrations used for modulating the purinosome were 20 μM, 25 μM, 100 nM, and 1 μM for DMAT, TBB, oxymetazoline, and salmeterol, respectively. Control experiments were also carried out with 2 μL DMSO (*i.e.* 0.1% DMSO in final working solution).

DMR Assay

HeLa cells maintained in purine-rich medium were typically seeded in the biosensor microplate at 2 to 2.5 × 10^4 cells per well at passage 3 to 15 suspended in 50 μl of purine-rich medium, and were cultured at 37°C under 5% CO_2 for ~1 day to reach ~100% confluency. For toxin treatment, PTX was directly added to reach a final concentration of 100 ng/ml in the biosensor cell assay plates and then incubated overnight prior to assay. CTX was added to reach a final concentration of 400 ng/ml for 3 hrs prior to assay. To knockdown human CK2α catalytic subunits in HeLa cells, we carried out transient transfection with a plasmid expressing a verified siRNA, and confirmed the degree of CK2 knockdown using Western blotting[11] (Supplementary Methods). The cells were then washed twice with HBSS before DMR assays. Epic® wavelength interrogation system (Corning

Inc., Corning, NY) was used to record DMR. This system consists of a temperature-control unit (28°C), an optical detection unit and an on-board liquid handling unit with robotics. The detection unit is based on integrated fiber optics and enables kinetic measures of cellular responses with a time interval of ~15 sec. Solutions of small molecules were made by diluting the stored concentrated solutions with HBSS and transferred into a 384-well polypropylene compound storage plate to prepare a compound source plate. Two compound source plates were made separately when a two-step assay was performed. Both cell and compound source plates were incubated within the Epic system to reach thermal equilibrium (~1 hr). After a 2 min baseline was recorded, compounds were transferred using the on-board liquid handler. For screening endogenous GPCRs, the agonist dose was examined at 10 μM for organic molecules and 1 μM for both peptides and lipids.

Quantitative real-time PCR

Total RNA was extracted from HeLa cells using an RNeasy mini kit (Qiagen, Cat#74104). To eliminate genomic DNA contamination, on-column DNase digestion was performed using RNase-free DNase set (Qiagen, Cat#79254). The concentration and quality of total RNA were determined using a Nanodrop 8000 (Thermo Scientific). Customized PCR-array plates for 352 GPCR genes and reagents were ordered from SABiosciences. About 1 μg total RNA was used for each 96-well PCR-array. The PCR-array was performed on an ABI 7300 Real-Time PCR System following the manufacturer's instructions.

Calculations and data analysis

Quantification of DMR was performed by the real response at a specific time point for the dose responses induced by adrenergic receptor ligands (50min post-stimulation) and DMAT (10 min post-stimulation) (Fig.1f, Fig.2, Fig.3c), except for TBB whose N-DMR amplitude (the difference between its peak response and the response at 50 min post-stimulation) was calculated (Fig.1f, Fig.2). All DMR signals was buffer and solvent corrected. EC_{50} values were determined using nonlinear regression with GraphPad Prism 4.0 (GraphPad Software).

Statistical analysis

For screening, two independent measurements, each with duplicate, were performed and used to calculate the averaged responses. For dose responses, at least two independent measurements, each with at least duplicate, were performed to calculate the mean responses and the standard deviations (s.d.). The robustness of screening assays was calculated based on the coefficient of variation (CV) of and the difference between the positive controls and the negative controls (*i.e.*, the vehicle only) (n =48 for each). The Z factor was calculated using the formula of [1 – (3 × CV of the positive + 3 × CV of the negative)/(the mean of the positive – the mean of the negative)]. The Z factor > 0.5 was considered robust. For DMR assays using RNAi knockdown, two independent measurements, each with at least four replicates, were used to calculate the RNAi knockdown effects. A P value <0.05 was considered statistically significant.

Supplementary Material

Refer to Web version on PubMed Central for supplementary material.

Acknowledgments

This work was funded by National Institutes of Health; GM24129 (S.J.B.).

References

1. Neves SR, Ram PT, Iyengar R. G protein pathways. Science. 2002; 296:1636–1639. [PubMed: 12040175]
2. Pierce KL, Premont RT, Lefkowitz RJ. Seven-transmembrane receptors. Nat Rev Mol Cell Biol. 2002; 3:639–650. [PubMed: 12209124]
3. Dorsam RT, Gutkind JS. G-protein-coupled receptors and cancer. Nat Rev Cancer. 2007; 7:79–94. [PubMed: 17251915]
4. Rozengurt E. Mitogenic signaling pathways induced by G protein-coupled receptors. J Cell Physiol. 2007; 213:589–602. [PubMed: 17786953]
5. Rajagopal S, Rajagopal K, Lefkowitz RJ. Teaching old receptors new tricks: biasing seven-transmembrane receptors. Nat Rev Drug Discov. 2010; 9:373–386. [PubMed: 20431569]
6. Kroemer G, Pouyssegur J. Tumor cell metabolism: cancer's Achilles' heel. Cancer Cell. 2008; 13:472–482. [PubMed: 18538731]
7. Kaelin WG Jr, Thompson CB. Q&A: Cancer: clues from cell metabolism. Nature. 2010; 465:562–564. [PubMed: 20520704]
8. Denkert C, et al. Metabolite profiling of human colon carcinoma deregulation of TCA cycle and amino acid turnover. Mol Cancer. 2008; 7:72. [PubMed: 18799019]
9. Christopherson RI, Lyons SD, Wilson PK. Inhibitors of *de novo* nucleotide biosynthesis as drugs. Acc Chem Res. 2002; 35:961–971. [PubMed: 12437321]
10. An S, Kumar R, Sheets ED, Benkovic SJ. Reversible compartmentalization of *de novo* purine biosynthetic complexes in living cells. Science. 2008; 320:103–106. [PubMed: 18388293]
11. An S, Kyoung M, Allen JJ, Shokat KM, Benkovic SJ. Dynamic regulation of a metabolic multi-enzyme complex by protein kinase CK2. J Biol Chem. 2010; 285:11093–11099. [PubMed: 20157113]
12. An S, Deng Y, Tomsho JW, Kyoung M, Benkovic SJ. Microtubule-assisted mechanism for functional metabolic macromolecular complex formation. Proc Natl Acad Sci USA. 2010; 107:12872–12876. [PubMed: 20615962]
13. Fang Y, Ferrie AM, Fontaine NH, Yuen PK. Characteristics of dynamic mass redistribution of epidermal growth factor receptor signaling in living cells measured with label-free optical biosensors. Anal Chem. 2005; 77:5720–5725. [PubMed: 16131087]
14. Fang Y, Li G, Ferrie AM. Non-invasive optical biosensor for assaying endogenous G protein-coupled receptors in adherent cells. J Pharmacol Toxicol Methods. 2007; 55:314–322. [PubMed: 17207642]
15. Schroder R, et al. Deconvolution of complex G protein-coupled receptor signaling in live cells using dynamic mass redistribution measurements. Nat Biotechnol. 2010; 28:943–949. [PubMed: 20711173]
16. Fang Y. Label-free receptor assays. Drug Discov Today Technol. 2010; 7:E5–E11. [PubMed: 21221420]
17. Duncan JS, et al. An unbiased evaluation of CK2 inhibitors by chemoproteomics: characterization of inhibitor effects on CK2 and identification of novel inhibitor targets. Mol Cell Proteomics. 2008; 7:1077–1088. [PubMed: 18258654]
18. Pagano MA, et al. The selectivity of inhibitors of protein kinase CK2: an update. Biochem J. 2008; 415:353–365. [PubMed: 18588507]
19. Bylund DB, et al. International Union of Pharmacology nomenclature of adrenoceptors. Pharmacol Rev. 1994; 46:121–136. [PubMed: 7938162]
20. Morris AJ, Malbon CC. Physiological regulation of G protein-linked signaling. Physiol Rev. 1999; 79:1373–1430. [PubMed: 10508237]

21. Baker JG. The selectivity of beta-adrenoceptor antagonists at the human β_1, β_2 and β_3 adrenoceptors. Br J Pharmacol. 2005; 144:317–322. [PubMed: 15655528]
22. Barbieri JT, Cortina G. ADP-ribosyltransferase mutations in the catalytic S-1 subunit of pertussis toxin. Infect Immun. 1988; 56:1934–1941. [PubMed: 3135265]
23. Gill DM, Meren R. ADP-ribosylation of membrane proteins catalyzed by cholera toxin: basis of the activation of adenylate cyclase. Proc Natl Acad Sci USA. 1978; 75:3050–3054. [PubMed: 210449]
24. Hanyaloglu AC, et al. Casein kinase II sites in the intracellular C-terminal domain of the thyrotropin-releasing hormone receptor and chimeric gonadotropin-releasing hormone receptors contribute to beta-arrestin-dependent internalization. J Biol Chem. 2001; 276:18066–18074. [PubMed: 11278484]
25. Musnier A, Blanchot B, Reiter E, Crepieux P. GPCR signalling to the translation machinery. Cell Signal. 2010; 22:707–716. [PubMed: 19887105]
26. Rebholz H, et al. CK2 negatively regulates $G_{\alpha s}$ signaling. Proc Natl Acad Sci USA. 2009; 106:14096–14101. [PubMed: 19666609]
27. Torrecilla I, et al. Phosphorylation and regulation of a G protein-coupled receptor by protein kinase CK2. J Cell Biol. 2007; 177:127–137. [PubMed: 17403928]
28. Gao Y, Wang HY. Casein kinase 2 Is activated and essential for Wnt/β-catenin signaling. J Biol Chem. 2006; 281:18394–18400. [PubMed: 16672224]

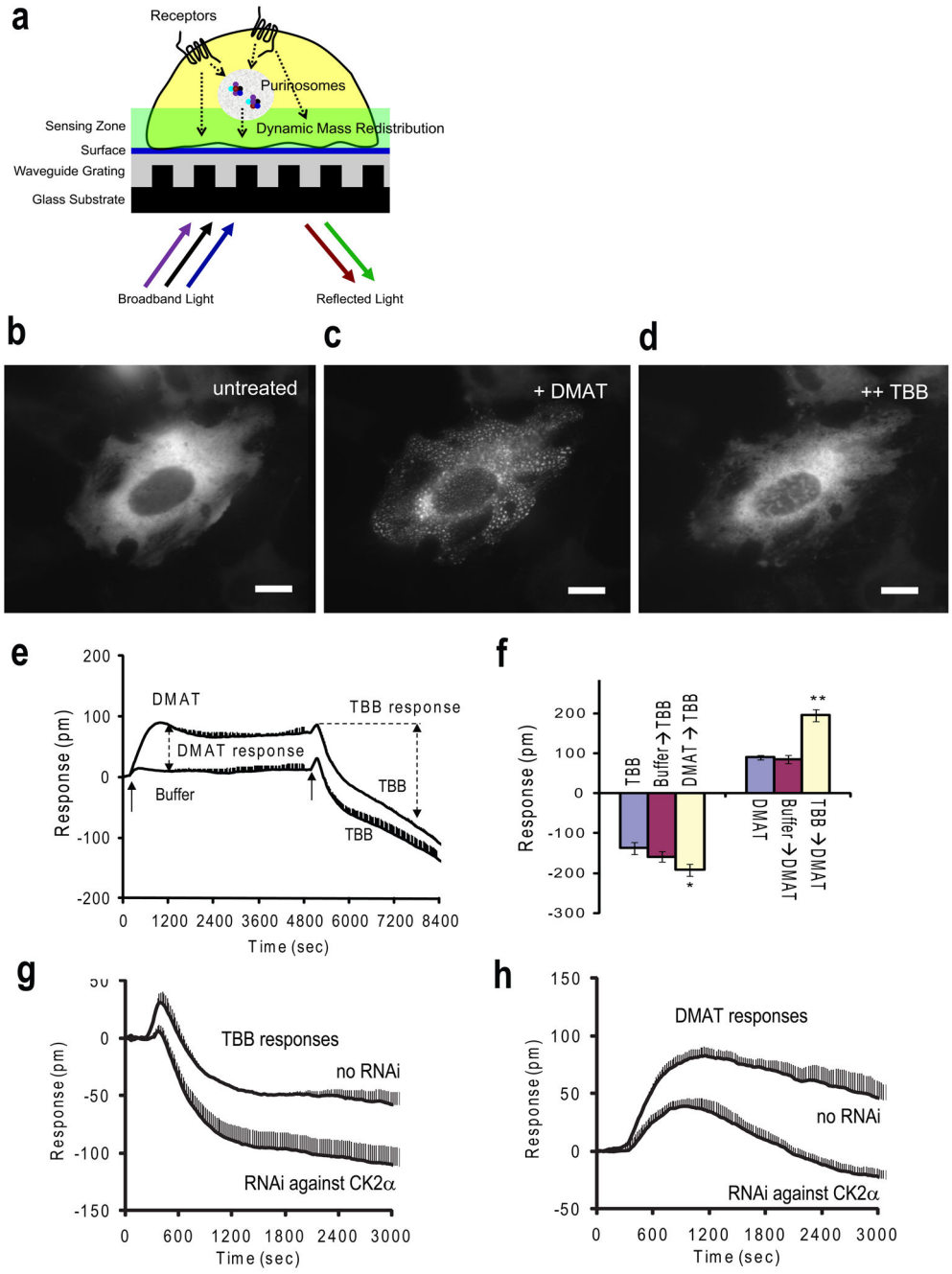

Figure 1.

Characteristic signatures of purinosome assembly/disassembly observed by fluorescent live-cell imaging and DMR assays. (**a**) Principle of DMR assays using a RWG biosensor. Ligand-mediated purinosome assembly/disassembly causes redistribution of cellular contents, resulting in shifts in resonant wavelength, which, in turn, lead to characteristic DMR. (**b**–**d**) A representative set of fluorescent images of hFGAMS-GFP in the same HeLa cell obtained after sequential additions of DMAT and TBB to a purine-rich medium: (**b**) prior to addition of DMAT, (**c**) 1 hr after treatment with DMAT (20 μM), (**d**) an additional 1 hr after successive treatment with TBB (25 μM). Scale bar, 10 μm. (**e**) The DMR of a HeLa

cell layer induced by DMAT (10μM) or the vehicle (buffer), followed by TBB (25μM). Broken arrows indicate the responses used for calculating the DMR amplitudes of DMAT (10 min post-stimulation) and TBB (50min post-stimulation). Solid arrows indicate the time when a compound was added. Data represent mean values ± s.d. (4 independent measurements, each with 3 replicates). (**f**) Cross-potentiation between the DMAT (10 μM) and TBB (25 μM) responses. * *p* value < 0.05 versus the other two conditions. n = 4. ** *p* value < 0.001 versus the other two conditions. Data represent mean values ± s.d. (3 independent measurements, each with 4 replicates). (**g–h**) The effect of CK2α siRNA knockdown on the DMR of TBB (**g**) or DMAT (**h**). Mock transfection was the control (no RNAi). Data represent mean values ± s.d. (2 independent measurements, n = 8).

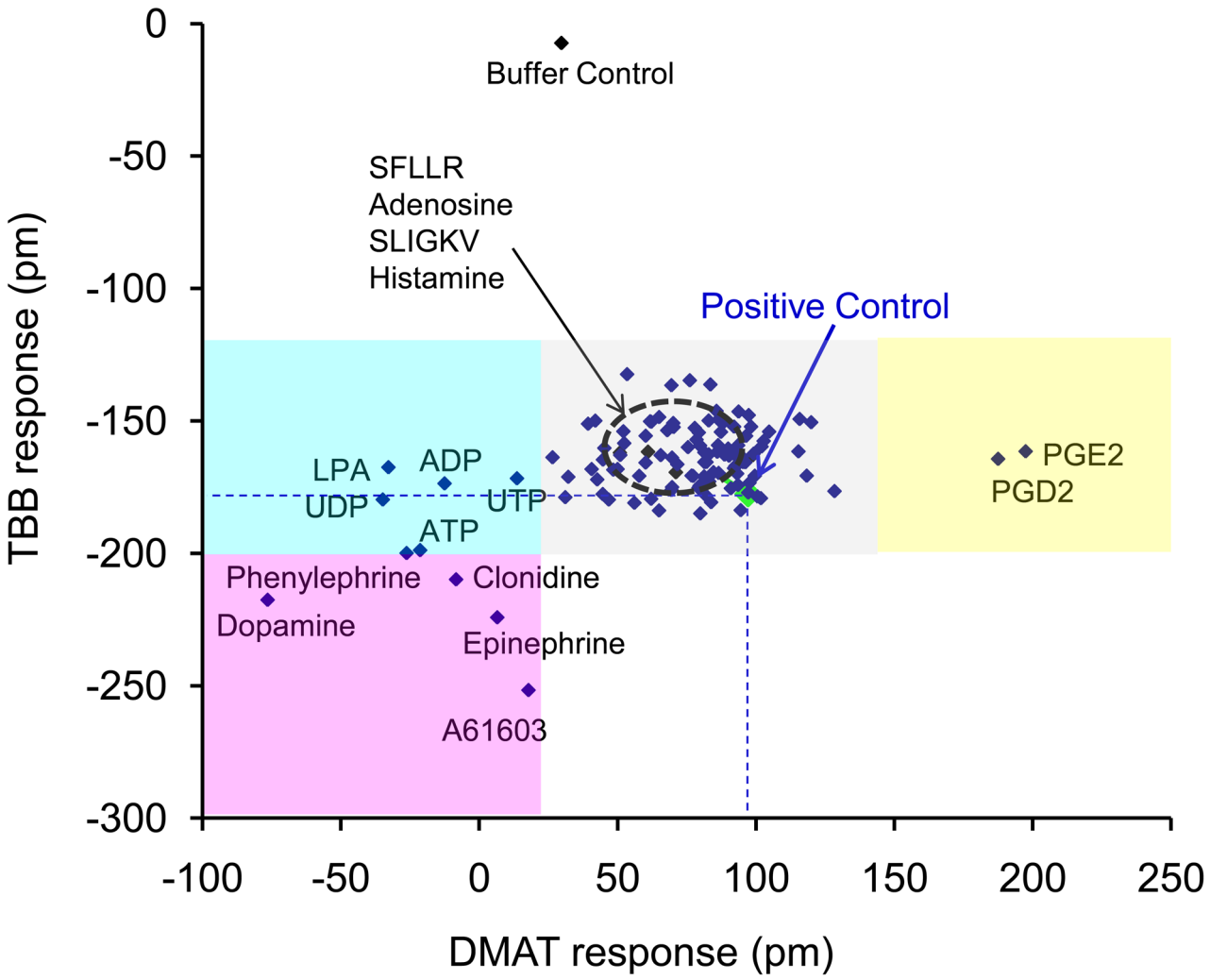

Figure 2.

DMAT and TBB responses after pretreatment of HeLa cells with a GPCR agonist library. DMAT responses were plotted on the *x*-axis against TBB responses on the *y*-axis. Data represent mean values (2 independent measurements, each in duplicate).

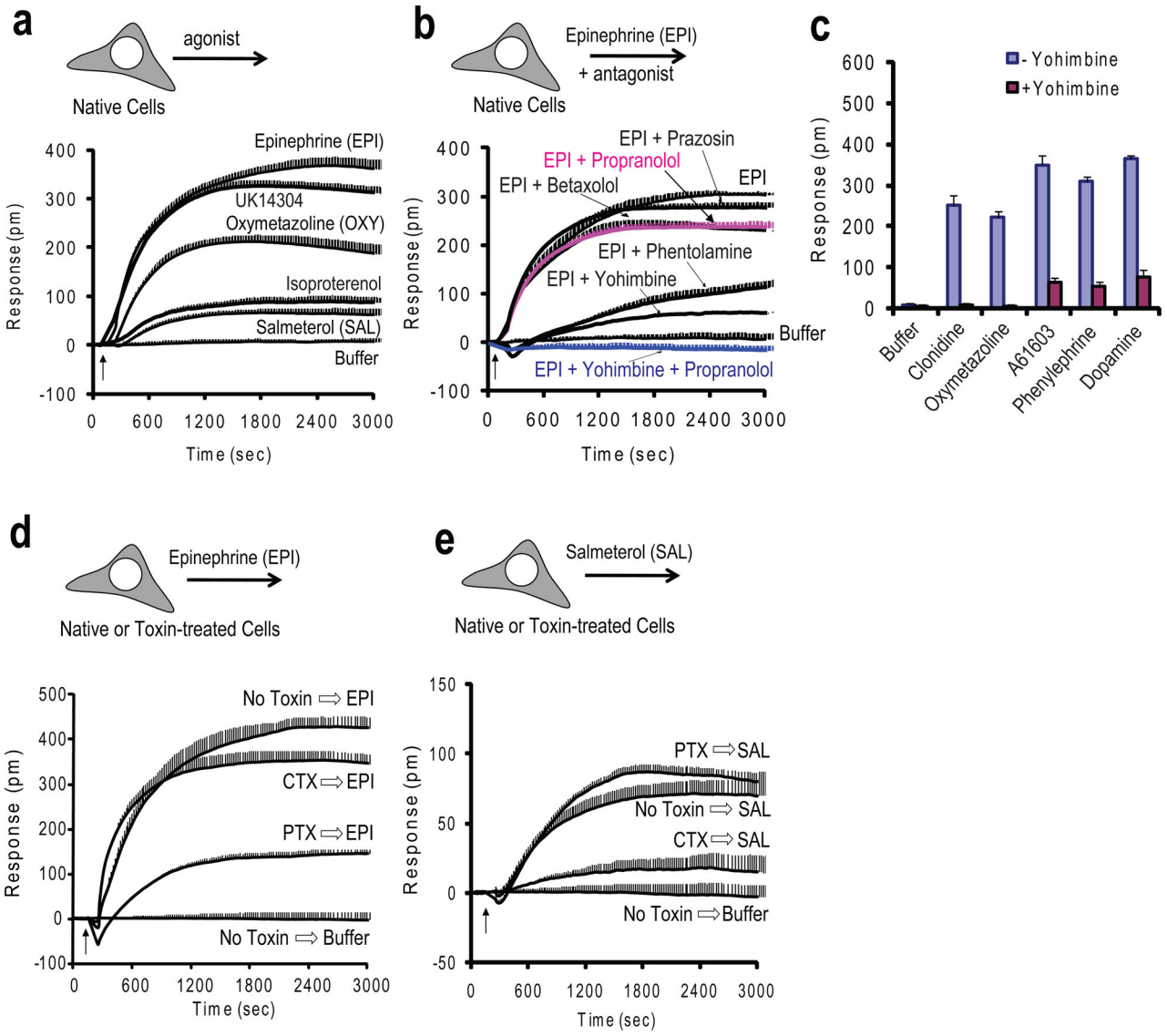

Figure 3. DMR assays characterizing endogenous adrenergic receptors manipulated by corresponding agonists, antagonists and toxins

(**a**) DMR signals from the monolayer HeLa cells induced by either epinephrine (EPI, 128 nM), UK14304 (100 nM), oxymetazoline (OXY, 128 nM), salmeterol (SAL, 4 μM), isoproterenol (10 μM) or the vehicle only (Buffer). Data represent mean values ± s.d. (2 independent measurements, n = 12). (**b**) The DMR signals of EPI in the presence and the absence of antagonists. All the tested antagonists, prazosin, propranolol, betaxolol, phentolamine and yohimbine, were assayed at 10 μM in the presence of EPI (100 nM). Data represent mean values ± s.d. (2 independent measurements, n = 12). (**c**) The impact of yohimbine on the DMR signals induced by distinct AR agonists. The P-DMR amplitudes at 50min post stimulation were calculated. Data represent mean values ± s.d. (2 independent measurements, n = 12). (**d–e**) DMR signals of different ligands with and without toxin pretreatment: EPI (10 μM) (**d**) and SAL (4 μM) (**e**) were used. PTX was at 100 ng/ml and

CTX at 400 ng/ml. An arrow indicates a time point when a last molecule was added to the cells. Data represent mean values ± s.d. (2 independent measurements, n = 4).

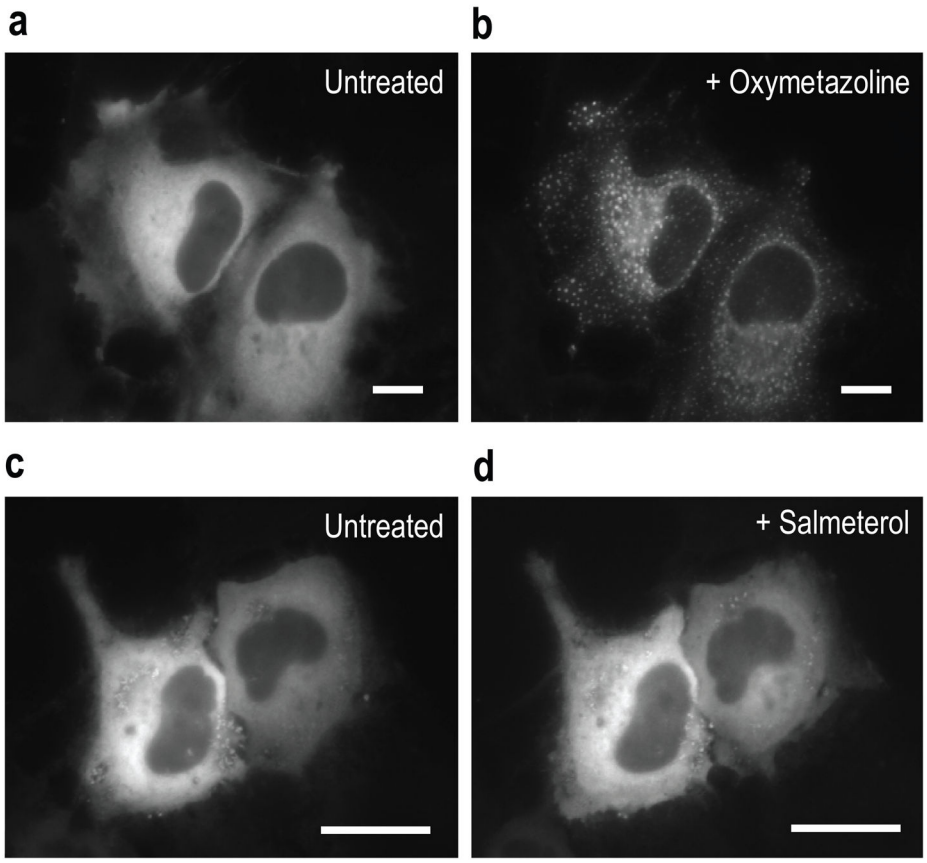

Figure 4.

Oxymetazoline, but not salmeterol, promoted purinosome formation in live HeLa cells. Oxymetazoline (100 nM) or salmeterol (1 μM) was supplied to HeLa cells transiently expressing hFGAMS-GFP as a purinosome marker. Individual images were obtained prior to the drug addition (untreated; **a** and **c**) and after the cells had been incubated with oxymetazoline (**b**) or salmeterol (**d**) for ~90 min. Scale bars, 10 μm.

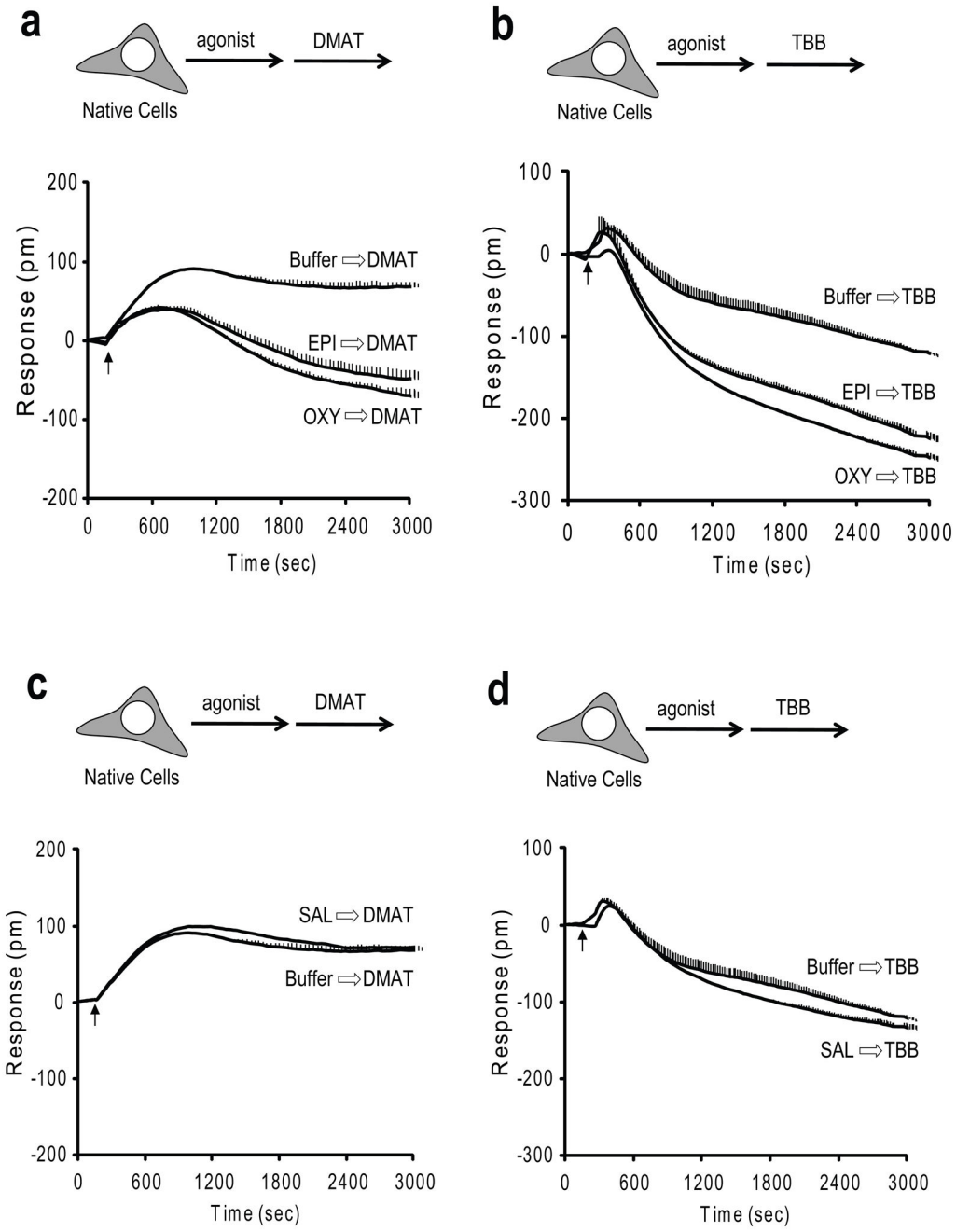

Figure 5. Activation of α_{2A}-AR, but not β_2-AR, influenced purinosome assembly

(**a–b**) DMR signals from 20 μM of DMAT (**a**) or 25 μM of TBB (**b**) in HeLa cells pretreated with buffer, EPI (128 nM) or OXY (128 nM) for 1 hr. Data represent mean values ± s.d. (2 independent measurements, n = 4). (**c–d**) DMR signals from 20 μM of DMAT (**c**) or 25 μM of TBB (**d**) for HeLa cells pretreated with buffer or SAL (4 μM). Data represent mean values ± s.d. (2 independent measurements, n = 4). An arrow indicates a time point when a last molecule was added to the cells.

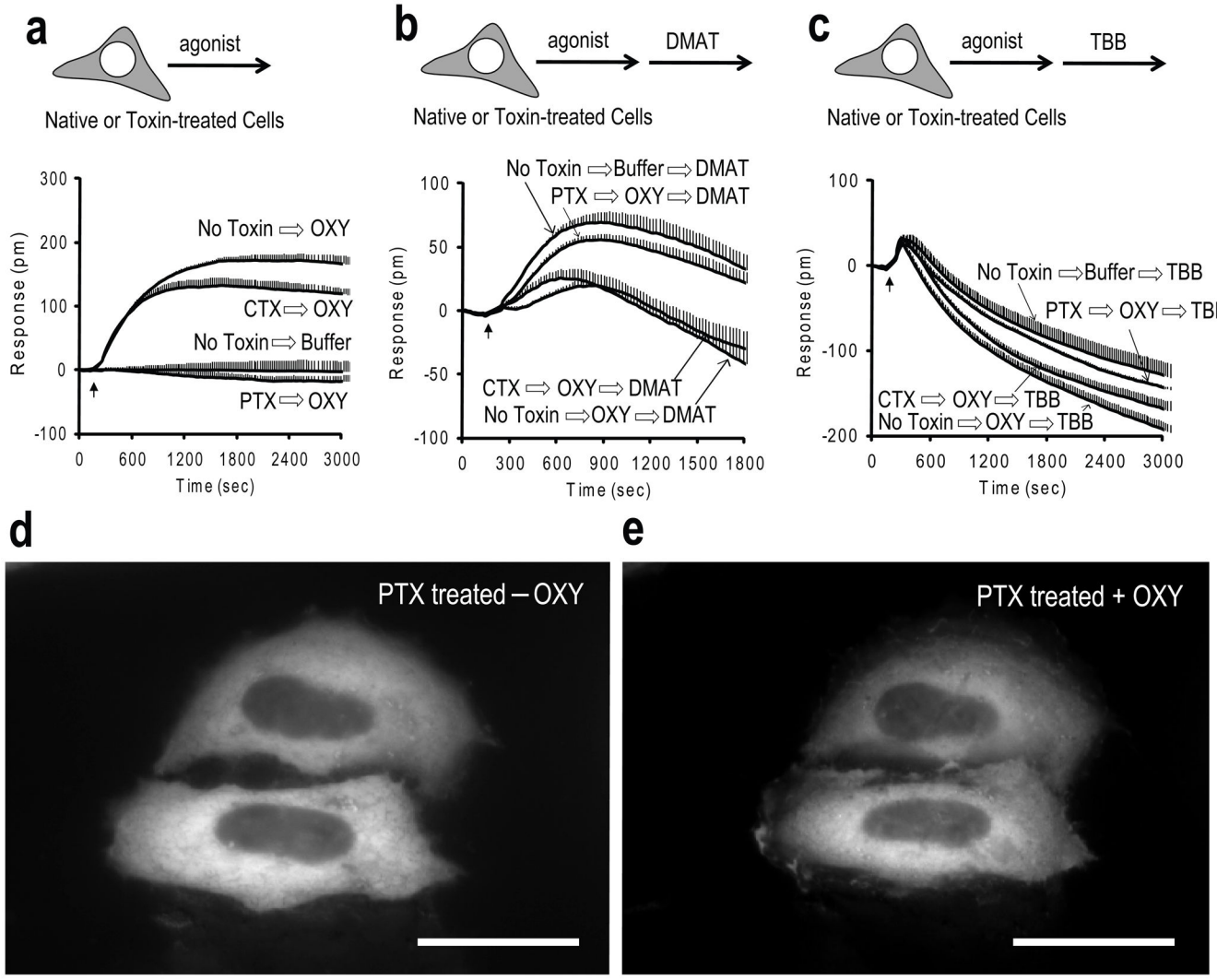

Figure 6. $G_{\alpha i}$ signaling for purinosome regulation by α_{2A}-AR activation

(**a**) DMR signals were induced by OXY (10 μM) in untreated, PTX- or CTX-treated HeLa cells. Treatment with the vehicle only (buffer) was also included as a negative control. Data represent mean values ± s.d. (2 independent measurements, n = 4). (**b–c**) After sequential pretreatments of toxins and OXY (10 μM, 1 hr) in HeLa cells, DMR signals were monitored upon treatment with 20 μM of DMAT (**b**) or 25 μM of TBB (**c**). Data represent mean values ± s.d. (2 independent measurements, n = 4). (**d–e**) PTX-pretreated HeLa cells expressing hFGAMS-GFP under purine-rich medium did not promote purinosome clusters even after 3 hr incubation with 100 nM of OXY. An arrow indicates a time point when a last molecule was added to the cells. Scale bars, 10 μm.